

New Equations for Describing Contact Area between Tire and Ground

CUI Zhibo^{1,2}, SU Zhaoqian², HOU Dandan³, ZHANG Chunsheng³, WANG Youshan², LIU Yuyan¹, WU Jian²

(1. Key Laboratory of the Ministry of Industry and Information Technology, New Energy Conversion and Critical Material Storage Technology, Harbin Institute of Technology, Harbin 150001, China; 2. National Key Laboratory of Science and Technology on Advanced Composites in Special Environments, Harbin Institute of Technology, Harbin 150001, China; 3. Zhongce Rubber Group Co., Ltd, Hangzhou 310018, China)

Abstract: New equations are proposed to describe the shapes and sizes of the contact areas between tire and ground (the contact areas) under the conditions of static load, slip, camber, and rolling. The equations are super ellipse and trigonometric function with four parameters. Results indicate that the contact areas under the conditions of static load, slip, camber can be well described by super ellipse, in the most complicated case, fourteen parameters are used. The rolling contact area can be reconstructed by the trigonometric function completely. Symmetrical and asymmetrical shapes can both be described perfectly. The suggested curves will make calculate size of the areas easily. The described shapes and sizes are in good agreement with the measured, the maximum deviation is only 2.88%. This work will provide an instrument for understanding the contact area and be helpful for analyzing tire and road.

Key words: contact areas; contact shape; tire and ground; super ellipse; equation

CLC number: TQ336.1

Document code: A

Article ID: 1000-890X(2020)09-0670-07

DOI: 10.12136/j.issn.1000-890X.2020.09.0670



OSID开放科学标识码
(扫码与作者交流)

There are three characteristics of the tire contacting with ground, the contact areas between the tire and ground (the contact area) is one of them, including shape and size of the area^[1]. As an important factor of the tire and vehicle, the contact area affects the traction, braking, cornering and wear performances^[2]. The contact area can be affected by structures, deflection of the tire, the operating conditions of the vehicle and the properties of the ground^[3-6], so it is very complicated. How to describe the contact area has been one of the research focuses^[5].

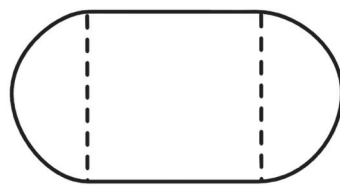
Fund projects: National Natural Science Foundation of China Project (51790502), Open Grant of National Key Laboratory of Science and Technology on Advanced Composites in Special Environments (JCKYS2019603C016)

Author brief introduction: Cui zhibo (1987—), male, from Chengde city, Hebei province, PhD., mainly engaged in the research of tire structure design.

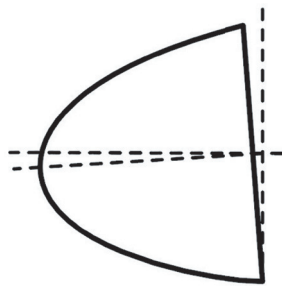
E-mail: cuizhibo1987@163.com

The contact area between the bias tire and hard road can be well described by ellipse, especially the tire has large deformation^[7]. When the deformation is relatively small, the contact area may be described by a circle. The ellipses were also used to describe the contact areas of tractor tires^[8], aircraft tires^[9], and plate tests^[10-11]. In general, the contact area between the radial tire and ground is not an ellipse apparently, a rectangle with rounded ends was used to describe it, and half circles were used as the rounded ends usually^[12]. Because of using multiple curves to describe the contact area is not convenient, super ellipse was used to replace the curves, it can be a circle, ellipse or rectangle if the exponent is appropriately changed, and it was used to describe the contact area of agricultural tires^[7, 13]. The sizes of the areas (A) can be calculated according to the curves, for a circle is $A = \pi r^2$ (r is the radius of the circle), for a rectangle

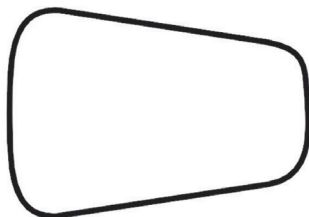
is $A = cd$ (c and d are the length and width of the rectangle respectively), for an ellipse is $A = \pi ab$ (a and b are the half length of the major axes), for a super ellipse is a numerical integral, and for the multiple curves is the sum of each part^[12]. The sizes of the contact area can also be measured^[3, 14]. Most simple contact areas can be described by the curves introduced above, and the sizes can be calculated easily. However, some areas are a little complicated, and they can not be depicted by the introduced curves, such as Fig. 1.



(a) Under static load



(b) With a slip angle



(c) With a camber angle



(d) Rolling with a speed

Fig. 1 The contact shape between the tire and ground

The characters of the contact shape in Fig. 1 (a) are that there are long straight lines in longitudinal direction, however, arc lines in width direction. The contact shape is incongruous in the length and width direction apparently. In general, the contact area between the radial tire and hard road under static load will be similar to Fig. 1 (a), and the shapes were introduced in literatures [8] and [15-17].

The shape similar to Fig. 1 (b) is introduced in literature [1]. The contact shape of the tire and ground with a camber angle is similar to Fig. 1 (c), the shapes similar to these were obtained by literatures [18-22]. They are different from Fig. 1 (a), the shapes do not have two parallel edges, and they have angles with the traveling directions of tires.

Fig. 1 (d) is a contact area that the tire is rolling with a speed, one of the major axes of the area is not passing through the center of the contact area, and there are waves in the front of the contact area and two straight lines in the width direction, the contact shapes similar to this were obtained by literature [1].

In this paper, new equations are introduced to describe the contact shapes under various conditions, and the methods of calculating the contact shapes sizes are proposed. Some practical implementations are done to verify the equations.

1 Shape described model

1.1 Super ellipse equation

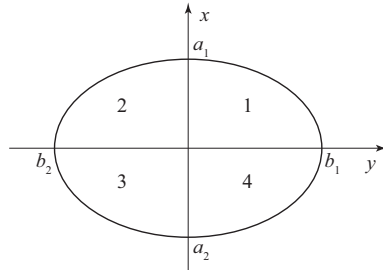
U. Hallonborg^[7] used super ellipse to describe the contact area, the equation of super ellipse is given by

$$\left(\frac{x}{a}\right)^n + \left(\frac{y}{b}\right)^n = 1 \tag{1}$$

where n is the exponent, x and y are the coordinate values of the points on the curves.

When $n=2$, the curve is an ellipse, when $n \rightarrow \infty$, it is a rectangle, when $a=b=1$ and $n=2$, it becomes

a circle. If the values of a and b are given, the shapes are controlled by n . The coordinate system and sub-regions of the contact areas are shown in Fig. 2.



1—First quadrant, 2—Second quadrant, 3—Third quadrant, 4—Fourth quadrant.

Fig. 2 The coordinate system and sub-regions of the contact area

In Fig. 2, the shape is divided into four sub-regions, which are in four quadrants. In order to describe asymmetric geometry, a_1 is not necessarily equal to a_2 , and b_1 is also not necessarily equal to b_2 . However, in order to guarantee the continuity of the curve, there must be the same value of a_1 and a_2 (or b_1 and b_2) in the boundary of two quadrants. At this time, there are $a_1 = a_2 = a$ and $b_1 = b_2 = b$.

1.2 Equations for describing the contact areas

In order to describe the shapes like Fig. 1 (a) and Fig. 1 (b), the Eq. (1) can be revised by

$$\left(\frac{x}{a}\right)^m + \left(\frac{y}{b}\right)^n = 1 \tag{2}$$

where m is exponent, m and n are positive real numbers.

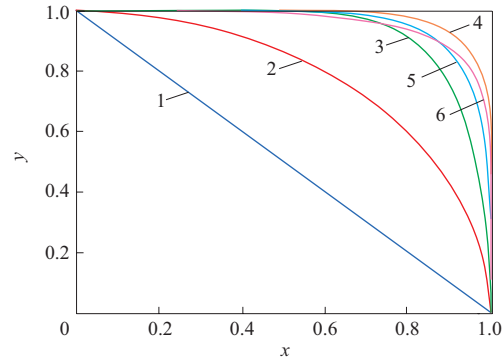
When a, b, m and n have different values, the curve will become different shapes, as shown in Table 1.

Exponent n affects the distance between the

Table 1 The curve changes with different values of a, b, m and n

a	b	m	n	Curve
$a > 0$	$b > 0$	2	2	Ellipse
$a = b > 0$	$b = a > 0$	2	2	Circle
$a > 0$	$b > 0$	∞	∞	Rectangle
$a > 0$	$b > 0$	$m = n$		Super ellipse

curve and x axis, and exponent m affects the distance between the curve and y axis. The curves with different values of m and n when $a = b = 1$ are shown in Fig. 3.



m/n : 1—1/1, 2—2/2, 3—8/2, 4—8/8, 5—8/4, 6—4/8.

Fig. 3 The curves of Eq.(2) in the first quadrant with different values of m and n when $a = b = 1$

Fig. 3 shows that the higher the value of n , the closer the curve is to the line $y = b$, and the higher the value of m , the closer the curve is to the line $x = a$. Because of using m and n , not only n , Eq. (2) is able to describe more complicated shapes.

In order to make the Eq. (2) to be an explicit function to describe the contact area like Fig.1 (a) and (b), the coordinate system can be set as Fig.2, the curves in each quadrant can be expressed as Eq. (3—6). Eq. (3—6) are respectively in 1—4 quadrants.

$$y_1 = f(x_1) = b_1 \left[1 - \left(\frac{x_1}{a_1}\right)^{m_1} \right]^{\frac{1}{n_1}} \tag{3}$$

$$y_2 = f(x_2) = b_2 \left[1 - \left(-\frac{x_2}{a_1}\right)^{m_2} \right]^{\frac{1}{n_2}} \tag{4}$$

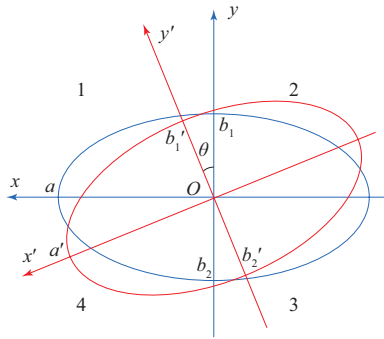
$$y_3 = f(x_3) = -b_2 \left[1 - \left(-\frac{x_3}{a_2}\right)^{m_3} \right]^{\frac{1}{n_3}} \tag{5}$$

$$y_4 = f(x_4) = -b_1 \left[1 - \left(\frac{x_4}{a_2}\right)^{m_4} \right]^{\frac{1}{n_4}} \tag{6}$$

where the subscripts of x, y, m, n denote quadrants, respectively.

For the contact shape like Fig. 1 (b), it can be divided into two parts rather than four parts, they are in the first and the fourth quadrant, and the shape may be symmetrical or asymmetrical.

The Eq. (2) can also be used to describe the shapes, and a new coordinate system should be built, such as Fig. 4. If the slip angle is opposite to the direction in Fig. 4, just changing x axis to the opposite direction.



The note is the same as Fig. 2.

Fig. 4 The coordinate system for the contact area with a slip angle

Where a (a') is the contact length of the area, b_1 (b_1') and b_2 (b_2') are the widest points from the x (x') axis in the boundaries of the contact area, θ is the steer angle.

If b_1 is not equal to b_2 , the contact shape is asymmetrical, if b_1 is equal to b_2 , the shape may be symmetrical or asymmetrical, because there are other two parameters also affect the curves, they are m and n in Eq. (2). In order to describe the contact shape, the Eq. (2) can be expressed as Eq. (7) (in the first quadrant) and Eq. (8) (in the fourth quadrant).

$$y_1 = f(x_1) = b_1 \left[1 - \left(\frac{x_1}{a} \right)^{m_1} \right]^{\frac{1}{n_1}} \quad (7)$$

$$y_4 = f(x_4) = -b_2 \left[1 - \left(\frac{x_4}{a} \right)^{m_4} \right]^{\frac{1}{n_4}} \quad (8)$$

A coordinate transformation can be used to make the curves to the coordinate system of x' and y' . The rule of coordinate transformation is

$$\begin{cases} x' = x \cos \theta + y \sin \theta \\ y' = x \sin \theta + y \cos \theta \end{cases} \quad (9)$$

Substituting Eq. (7—8) into Eq. (9), the curves can be expressed as Eq. (10) (in first quadrant)

and Eq. (11) (in fourth quadrant) in new coordinate system.

$$\begin{cases} x'_1 = x_1 \cos \theta + y_1 \sin \theta \\ y'_1 = x_1 \sin \theta + y_1 \cos \theta \end{cases} \quad (10)$$

$$\begin{cases} x'_4 = x_4 \cos \theta + y_4 \sin \theta \\ y'_4 = x_4 \sin \theta + y_4 \cos \theta \end{cases} \quad (11)$$

In order to describe the shape likes Fig. 1 (c), a new equation can be used by

$$y = d \left[\sin \left(\frac{\pi}{2a} x \right)^p \right] + b \quad (12)$$

where the meanings of a, b, d are shown in Fig. 5, p is the exponent, in general, its values ranges from 0 to 3.

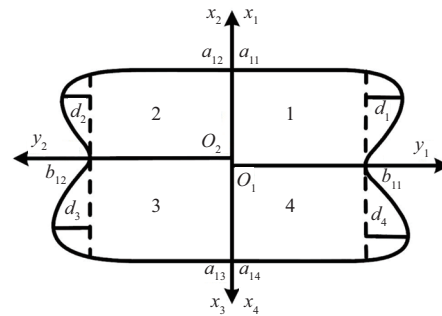


Fig. 5 The coordinate system for the contact shape when tire is rolling

The area is divided into four sub-regions, they are in four quadrants. As shown in Fig. 5, the values of a, b, d and p in one quadrant may be not equal to them in another quadrant. However, in order to avoid the discontinuity in the boundary of two quadrants, the sum of a_{11} and a_{14} should equal to the sum of a_{12} and a_{13} . The curves of Eq. (12) when $a = d = 1, b = 0$ and $p = 1.0, 1.5, 2.0, 2.5, 3.0$ are shown in Fig. 6.

In the Fig. 6, with the increase of p the curves become more curved, and the peaks are moving to the left.

For describing the contact area, the equation in each quadrant can be expressed as Eq. (13—16). Eq. (13—16) are respectively in 1—4 quadrants.

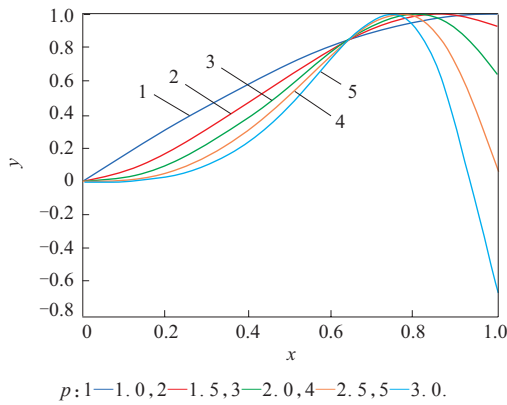


Fig. 6 Curves of Eq. (12) with different values of p when $a=d=1$ and $b=0$

$$y_1 = f(x_1) = d_1 \left[\sin\left(\frac{\pi}{2a_{11}} x_1\right)^{p_1} \right] + b_{11} \quad (13)$$

$$y_2 = f(x_2) = d_2 \left[\sin\left(\frac{\pi}{2a_{12}} x_2\right)^{p_2} \right] + b_{12} \quad (14)$$

$$y_3 = f(x_3) = d_3 \left[\sin\left(\frac{\pi}{2a_{13}} x_3\right)^{p_3} \right] + b_{12} \quad (15)$$

$$y_4 = f(x_4) = d_4 \left[\sin\left(\frac{\pi}{2a_{14}} x_4\right)^{p_4} \right] + b_{11} \quad (16)$$

where a_{11} and a_{14} are the distances from O_1 to upper and lower boundaries of the contact shape respectively, a_{12} and a_{13} are the distances from O_2 to upper and lower boundaries of the contact shape respectively. d_1-d_4 are the amplitudes of the waves in each quadrant. p_1-p_4 are the exponents of the curves in each quadrant.

From the Eq. (12—16), we know that all curves in the Fig. 6 pass through a same point, its position is $[2a/\pi, d \times \sin 1 + b]$.

2 Size of the contact area

The size of the contact area can be obtained by sum of the sizes in four quadrants, such as Eq. (17).

$$A = \sum_{i=1}^j A_i \quad (j=2 \text{ or } 4) \quad (17)$$

where A_i is the size of the area in one quadrant, subscript i is from 1 to 4, j is the quantity of parts that the contact area can be divided into. When the shapes are like Fig. 1 (a), (c) or (d), j can be chosen as 4, and when the shapes are like Fig. 1 (b),

j is equal to 2. For the shapes that can be described by Eq. (2) and Eq. (12), the size of the area in one quadrant can be obtained by integration of $y_i=f(x_i)$

$$A_i = \int_0^{a_i} y_i dx_i = \int_0^{a_i} f(x_i) dx_i \quad (18)$$

where $f(x_i)$ are the functions of describing the curves in each quadrant for different contact shapes, for example, the sizes of the areas that can be described by Eq. (12) are

$$A_i = \int_0^{a_i} f(x_i) dx_i = \int_0^{a_i} \left\{ d_i \left[\sin\left(\frac{\pi}{2a_i} x_i\right)^p \right] + b_i \right\} dx_i \quad (19)$$

The size of the area can be described by Eq. (2) is

$$A_i = \int_0^{a_i} f(x_i) dx_i = \int_0^{a_i} b_i \left[1 - \left(\frac{x_i}{a_i}\right)^{m_i} \right]^{\frac{1}{n_i}} dx_i \quad (20)$$

As the integrands are very complicated, there is no simple evaluation of the integral, and numerical methods must be used to calculate the integral.

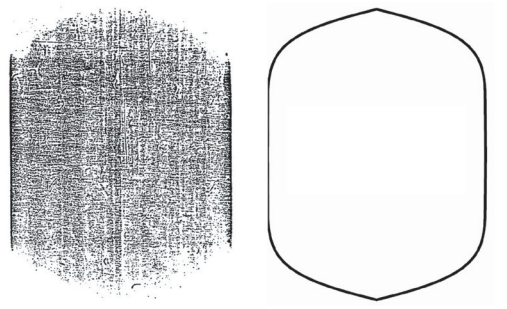
3 Practical implementations

Some practical examples that are based on literature [1, 2, 15, 17], their shapes and sizes are described and calculated using the equations in this paper. The results are shown in Fig. 7—12, and the errors of sizes between the investigated and described are also given, the method of the calculating errors (δ) is given by Eq. (21).

$$\delta = \frac{A_l - A_D}{A_l} \times 100\% \quad (21)$$

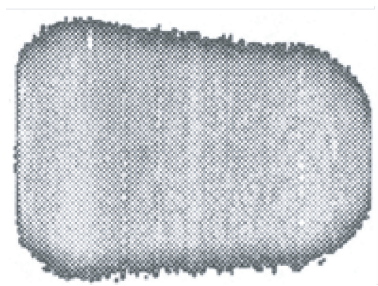
where A_l is the size of contact area in literature, A_D is the size of contact area described by equations in this paper.

The actual values of a_i and b_i of some contact areas are not given in the literatures, however, there is no effect on calculating the errors of sizes, and they can be seen to be enlarged or reduced proportionally. The shapes can also be seen to be enlarged or reduced proportionally, and the values of m_i and n_i will not change in the process, so, in some figures only the values of m_i and n_i are given.

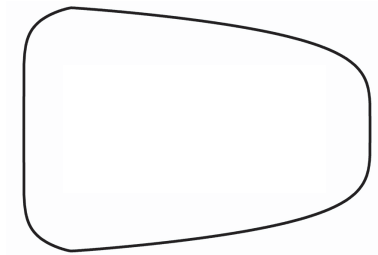


(a) The measured contact shape in literature[15] (b) The curve for describing the contact shape

Fig. 7 The symmetrical contact area

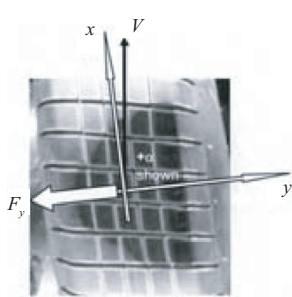


(a) The measured contact shape in literature[19]

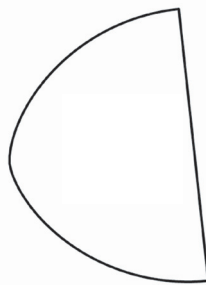


(b) The curve for describing the contact shape

Fig. 8 The monosymmetric contact shape when the tire has a camber angle

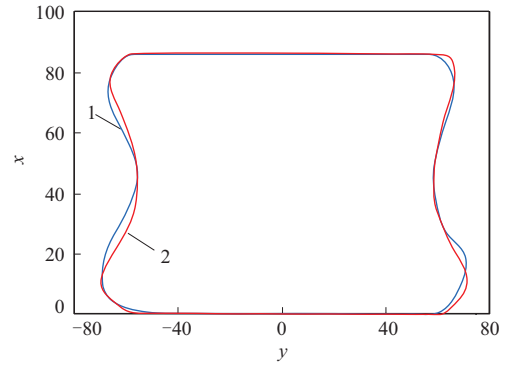


(a) The measured contact shape in literature[18]



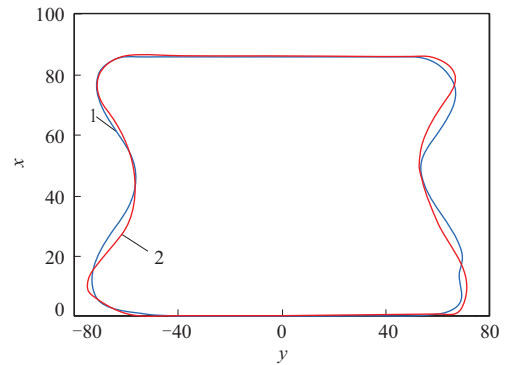
(b) The curve for describing the contact shape

Fig. 9 The area with a slip angle



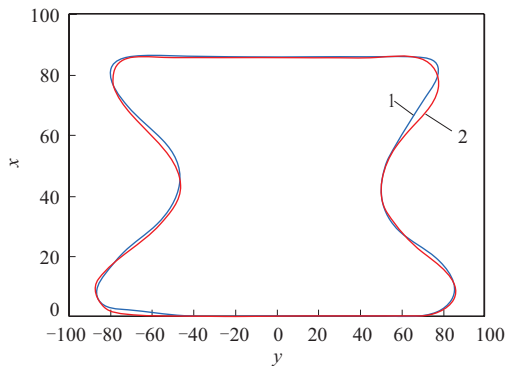
1— $V=30 \text{ km} \cdot \text{h}^{-1}$ in literature[1], 2—Fitting by Eq. (12).

Fig. 10 The contact area when tire is rolling with a speed of $30 \text{ km} \cdot \text{h}^{-1}$



1— $V=60 \text{ km} \cdot \text{h}^{-1}$ in literature[1], 2—Fitting by Eq. (12).

Fig. 11 The contact area when tire is rolling with a speed of $60 \text{ km} \cdot \text{h}^{-1}$



1— $V=120 \text{ km} \cdot \text{h}^{-1}$ in literature[1], 2—Fitting by Eq. (12).

Fig. 12 The contact area when tire is rolling with a speed of $120 \text{ km} \cdot \text{h}^{-1}$

The agreement between the investigated and described shapes are very good, there are only some deviations at the protruding parts of the boundaries.

The most error of size is 2.88% between measured and calculated areas, which is acceptable.

4 Conclusion

New equations are developed for describing the contact area. It can be seen that the results are very accurate, they are not only able to describe the contact shape under static conditions, but also under slip and rolling conditions. The curves can describe the contact area on soft ground and hard road. They can also describe the symmetric and asymmetric contact areas. The suggested curves will make calculate size of the areas easily, and it is helpful for integrating the pressure in the contact area.

In the further studies, the effects of tire structures on parameters of the equations will be studied, and the pressure distributions in contact area will be described by these equations. There will be a great help for tire engineers to control the contact area when designing a new tire.

References

- [1] Alan Browne, Ludema K C, Clark S K. Mechanics of Pneumatic Tires: Contact between the Tire and Roadway[M]. Washington: U. S. Government Printing Office, 1981.
- [2] Pottinger M G. Pneumatic Tire: Contact Patch (Footprint) Phenomena[M]. Washington: U. S. Department of Transportation, 2006.
- [3] Sharma A K, Pandey K P. A Review on Contact Area Measurement of Pneumatic Tyre on Rigid and Deformable Surfaces[J]. Journal of Terramechanics, 1996, 33 (2) : 53-64.
- [4] Diserens E. Calculating the Contact Area of Trailer Tyres in the Field[J]. Soil & Tillage Research, 2009, 10 (3) : 302-309.
- [5] Namjoo Moslem, Golbakhshi Hossein. Numerical Simulation of Tire/ Soil Interaction Using a Verified 3D Finite Element Model[J]. Journal of Central South University, 2014, 21 : 817-821.
- [6] Chen Y, Wang K J, Zhou W F. Evaluation of Surface Textures and Skid Resistance of Pervious Concrete Pavement[J]. Journal of Central South University, 2013, 20 : 520-527.
- [7] Hallonborg U. Super Ellipse as Tyre-Ground Contact Area[J]. Journal of Terramechanics, 1996, 33 : 125-132.
- [8] Upadhyaya S K, Wulfsohn D. Relationship between Tire Deflection Characteristics and 2-D Tire Contact Area[J]. Transactions of the Asae, 1990, 33 (1) : 25-30.
- [9] Kilner J R. Pneumatic Tire Model for Aircraft Simulation[J]. Journal of Aircraft, 2012, 19 (10) : 851-857.
- [10] Youssef A F A, Ali G A. Determination of Soil Parameters Using Plate Test[J]. Journal of Terramechanics, 1982, 19 (2) : 129-147.
- [11] Soltynski A. The Mobility Problem in Agriculture[J]. Journal of Terramechanics, 1979, 16 (3) : 139-149.
- [12] Komandi G. The Determination of the Deflection, Contact Area, Dimensions and Load Carrying Capacity for Driven Pneumatic Tires Operating on Concrete Pavement[J]. Journal of Terramechanics, 1976, 13 (1) : 15-20.
- [13] Keller T. A Model for the Prediction of the Contact Area and the Distribution of Vertical Stress below Agricultural Tyres from Readily Available Tyre Parameters[J]. Biosystems Engineering, 2005, 92 (1) : 85-96.
- [14] Yong R, Boonsinsuk P, Fattah E A. Tyre Load Capacity and Energy Loss with Respect to Varying Soil Support Stiffness[J]. Journal of Terramechanics, 1980, 17 (3) : 131-147.
- [15] Kurt M M, Ronald H W, Richard B C, et al. Experimental Investigation of Truck Tire Inflation Pressure on Pavement-Tire Contact Area and Pressure Distribution[R]. Texas: The University for Texas at Austin, Center for Transportation Research, 1985.
- [16] Pedro Yap. Truck Tire Types and Road Contact Pressures[C]. International Symposium on Heavy Vehicle Weights and Dimensions. Kelowna: UC Berkeley Transportation Library, 1989: 1-20.
- [17] Pottinger M G. Effect of Suspension Alignment and Modest Cornering on the Footprint Behavior of Performance Tires and Heavy Duty Radial Tires[J]. Tire Science and Technology, 1999, 27 (3) : 128-160.
- [18] Korunović N, Trajanović M, Stojković M. Finite Element Analysis of a Tire Steady Rolling on the Drum and Comparison with Experiment[J]. Strojniski Vestnik, 2011, 57 (12) : 888-897.
- [19] Koehne S H, Matute B, Mundt R. Evaluation of Tire Tread and Body Interactions in the Contact Patch[J]. Tire Science and Technology, 2003, 31 : 159-172.
- [20] Guan Y J, Zhao G Q, Cheng G. FEA and Testing Studies on Static Camber Performance of the Radial Tire[J]. Journal of Reinforced Plastics and Composites, 2007, 26 : 1921-1936.
- [21] Cheng G, Wang W, Zhao G, et al. Influence of Camber Angle on Rolling Radial Tire under Braking State[J]. Procedia Engineering, 2011, 15 : 4310-4315.
- [22] Smith N D. Understanding Parameters Influencing Tire Modeling[C]. Formula SAE Platform. Colorado: Colorado State University, 2004: 1-22.

Submitted date: 2020-06-13